

pH-(low)-insertion-peptide (pHLIP) translocation of membrane impermeable phalloidin toxin inhibits cancer cell proliferation

Ming An^a, Dayanjali Wijesinghe^b, Oleg A. Andreev^{b,1}, Yana K. Reshetnyak^{b,1}, and Donald M. Engelman^{a,1}

^aDepartment of Molecular Biophysics and Biochemistry, Yale University, P.O. Box 208114, New Haven, CT 06520; and ^bPhysics Department, University of Rhode Island, 2 Lippitt Road, Kingston, RI 02881

Contributed by Donald M. Engelman, September 27, 2010 (sent for review September 23, 2010)

We find that pH-(low)-insertion-peptide (pHLIP)-facilitated translocation of phalloidin, a cell-impermeable polar toxin, inhibits the proliferation of cancer cells in a pH-dependent fashion. The monomeric pHLIP inserts its C terminus across a membrane under slightly acidic conditions (pH 6–6.5), forming a transmembrane helix. The delivery construct carries phalloidin linked to its inserting C terminus via a disulfide bond that is cleaved inside cells, releasing the toxin. To facilitate delivery of the polar agent, a lipophilic rhodamine moiety is also attached to the inserting end of pHLIP. After a 3 h incubation at pH 6.1–6.2 with 2–4 μ M concentrations of the construct, proliferation in cultures of HeLa, JC, and M4A4 cancer cells is severely disrupted (>90% inhibition of cell growth). Treated cells also show signs of cytoskeletal immobilization and multinucleation, consistent with the expected binding of phalloidin to F actin, stabilizing the filaments against depolymerization. The antiproliferative effect was not observed without the hydrophobic facilitator (rhodamine). The biologically active delivery construct inserts into 1-palmitoyl-2-oleoyl-sn-glycero-3-phosphocholine lipid bilayers with an apparent pK_a of ~ 6.15 , similar to that of the parent pHLIP peptide. Sedimentation velocity experiments show that the delivery construct is predominantly monomeric (>90%) in solution under the conditions employed to treat cells (pH 6.2, 4 μ M). These results provide a lead for antitumor agents that would selectively destroy cells in acidic tumors. Such a targeted approach may reduce both the doses needed for cancer chemotherapy and the side effects in tissues with a normal pH.

drug delivery | hydrophilic drugs | cytoplasmic delivery | targeting acidity | targeted chemotherapy

Cancer chemotherapy is often limited by the toxic side effects of antineoplastic agents. Targeted therapy, including targeted drug delivery, can improve the therapeutic index by reducing side effects in healthy tissues, while reducing the overall dose by concentrating the drug in the targeted tissue. Some drug delivery systems, such as liposomes and polymers, can passively target tumors due to the enhanced permeation and retention (EPR) effect (1–3). However, the EPR effect is small or nonexistent for certain tumors (2, 4–6). Most molecular targeting strategies take aim at specific cancer biomarker proteins such as overexpressed cell surface receptors. Antibodies and other molecules (e.g., transferrin, folate) have been used as targeting ligands to bind to these receptors for the delivery of imaging or therapeutic agents to cancer cells (7, 8). However, many cancer biomarker receptors (e.g., ERBB2) are not uniquely expressed in cancer cells but also in certain healthy cells, leading to side effects in patients (9). Further, therapy based on the targeting of specific binding sites is hampered by the heterogeneity of tumors, especially the differences among cells within a tumor (10, 11). The lack of homogeneously expressed target biomarkers (among cancer cells) and the ease with which clonal selection of cancer cells can circumvent a single (or a few) targeted protein(s) could explain why molecular targeting approaches have had limited success against solid tumors (and are frequently associated with rapid development

of resistance) (9, 12). Therefore, it is important to ask whether other, more general, features of cancer physiology might be exploited for targeted therapy against solid tumors.

Acidosis is a property of tumor microenvironments that may serve as a general biomarker (13–15) and we have developed an approach to target cells in tissues with a low extracellular pH. Our strategy is based on the action of the pH (low) insertion peptide (pHLIP)—a water-soluble peptide derived from the transmembrane (TM) helix C of bacteriorhodopsin (16). At pH values above seven, pHLIP in solution partitions to the surface of a lipid bilayer without inserting, and at a slightly acidic pH it inserts with a pK_a of ~ 6 in vitro to form a TM helix (16). At concentrations below 7 μ M, pHLIP molecules predominantly exist as monomers in solution, and in the presence of lipid vesicles (lipid:pHLIP molar ratio > 250:1), the monomeric state is maintained throughout membrane association and insertion (17, 18). Unlike other membrane active peptides (14), pHLIP does not cause membrane leakage in any of the membrane associated states (17, 19). In addition, pHLIP has shown no toxicity to cells (at concentrations up to 10 μ M at pH 6.5 for 1 h or 16 μ M at pH 7.4 for 24 h) or animals (4 mg/kg in mice, followed for 2 mo) (20, 21). The insertion process is unidirectional (C terminus in), rapid (<2 min in lipid vesicles) and reversible (upon pH increase to >7) (17, 20, 22). The transition between the surface bound state and the inserted state is mediated by the protonation or deprotonation of Asp side chains in the TM region (16, 21). These unique properties prompted us to test both (D)- and (L)-pHLIP as tumor-imaging vehicles in mice. When the noninserting N-terminal end of pHLIP is conjugated to a near-IR fluorescent dye (e.g., Cy5.5, AlexaFluor 750) or to the positron emission tomography probe ⁶⁴Cu-1,4,7,10-tetra-aza-cyclododecane-*N,N',N'',N'''*-tetra-acetic acid, these pHLIP imaging constructs successfully targeted acidic tissues in vivo, including tumors, kidneys, and sites of inflammation (21, 23). In mouse implant models, pHLIP-dye constructs found tumors, defined their borders with a high degree of accuracy (24), and accumulated in them, even when the tumor was very small (i.e., visually undetectable, ≤ 1 mm) (21).

Given its properties, it may be possible to use pHLIP for targeted intracellular delivery of therapeutic agents. Under acidic conditions, the folding of pHLIP across a membrane (into a TM helix) is exothermic (by ~ 2 kcal/mole) (18), and the insertion can move C-terminal cargo molecules across a lipid bilayer (20, 25). The cargo can be conjugated to the inserting C terminus of pHLIP via an S–S disulfide bond that is cleaved inside cells, re-

Author contributions: M.A., O.A.A., Y.K.R., and D.M.E. designed research; M.A., D.W., O.A.A., and Y.K.R. performed research; M.A. contributed new reagents/analytic tools; M.A., D.W., O.A.A., Y.K.R., and D.M.E. analyzed data; and M.A., D.W., O.A.A., Y.K.R., and D.M.E. wrote the paper.

The authors declare no conflict of interest.

¹To whom correspondence may be addressed. E-mail: donald.engelman@yale.edu, reshetnyak@mail.uri.edu, or andreev@mail.uri.edu.

This article contains supporting information on-line at www.pnas.org/lookup/suppl/doi:10.1073/pnas.1014403107/-DCSupplemental.

leasing cargo into the cytoplasm. Among cargos that have been successfully delivered to the cytoplasm in this fashion are (i) fluorescent dyes (e.g., dansyl), (ii) phalloidin-TRITC (1.3 kDa with $\text{LogP} \approx -0.05$, where P is the octanol-water partition coefficient), (iii) peptide nucleic acid (2.5 kDa), and (iv) cyclic peptides (up to 850 Da with $\text{LogP} \approx -3$) (20, 25). The pHLIP-mediated intracellular delivery does not rely on receptor binding or endocytosis (20), rather, the cargo molecule is directly delivered across the lipid bilayer of the plasma membrane. Compared to receptor-targeted delivery of chemotherapeutic agents, this approach has three potential advantages: (i) it is not sensitive to the heterogeneous expression of receptors or antigens among cancer cells within a tumor, for example, pHLIP-mediated delivery would destroy active and quiescent malignant cells alike because they share a common acidic microenvironment; (ii) direct cytoplasmic delivery avoids endosomal trapping of drug payloads—a noted problem that can plague drug carriers that rely on endocytosis for cellular entry (26); and (iii) because this method is not limited by the number of targeted receptors, more copies of therapeutic agents may be delivered per cell than receptor-mediated approaches. Thus, we envision using pHLIP-mediated drug delivery to preferentially destroy tumor cells while sparing normal tissue. In this study, we quantitatively investigate the activity of phalloidin delivered into cancer cells, showing that pHLIP can deliver a molecule in sufficient amounts for biological efficacy. Because pHLIP is not toxic on its own, cargo delivery could also be applied therapeutic purposes other than cell killing.

Results

Phalloidin, a cytotoxin isolated from the Death Cap mushroom *Amanita phalloides*, binds tightly to actin filaments ($K_d < 40$ nM) and stabilizes them against depolymerization (27–29). Phalloidin is a polar, cell-impermeable, cyclic heptapeptide (Fig. 1). When a sufficient amount of phalloidin is microinjected into a cytoplasm, cell proliferation is inhibited (30). Previously, we found that phalloidin-TRITC (attached to the C terminus of pHLIP) is translocated across the plasma membrane of HeLa, JC (breast adenocarcinoma), and TRAMP (prostate) cancer cells in a

pH-dependent manner, inducing stabilization of the actin cytoskeleton and formation of multinucleated cells (20). However, these qualitative results were obtained with a heterogeneous construct in which pHLIP-Cys is photo-cross-linked to phalloidin-TRITC (a phalloidin-rhodamine conjugate) via a thiol-reactive aryl azide linker (i.e., S-[2-(4-azidosalicyl-amido)ethylthiol]-2-thiopyridine), and no study of dosing was done. Our earlier synthetic approach was convenient for initial test experiments, but it is unsuitable for further studies because it results in an undefined mixture of products, partly due to the photo-cross-linking chemistry, and partly due to the fact that phalloidin-TRITC 4 is a mixture of stereo- and regioisomers (see Fig. 1 for its structural variations) (31). Here we present controlled studies using pure constructs.

Design and Syntheses of Delivery Constructs pHLIP-C(aminophalloidin) and pHLIP-K(rhodamine)-C(aminophalloidin)

To evaluate the therapeutic potential of phalloidin as a pHLIP-delivered cytotoxin, we need to use a chemically defined agent. Thus, we synthesized a single isomer pHLIP-C(aph) 5 in which aminophalloidin (aph) is directly attached to the C terminus Cys via a short disulfide linker (Fig. 1). The synthesis of pHLIP-C(aph) 5 begins with the commercially available single isomer aminophalloidin 2, which differs from phalloidin 1 only in that the terminal δ -hydroxyl group of side-chain 7 is replaced by an amino group (Fig. 1) (32). Treatment of aminophalloidin 2 with the bifunctional linker *N*-succinimidyl 3-(2-pyridyl-dithio)-propionate (SPDP) provides the pyridyl-disulfide-derivatized aminophalloidin PDP intermediate 3 (Fig. 1), which is subsequently conjugated to pHLIP-Cys via disulfide exchange to give the final construct 5. This two-step procedure was carried out without purification of intermediate 3. To avoid side reactions and to simplify purification, near quantitative amounts of SPDP (1.2 eq) and pHLIP-Cys (1.21 eq) were added. HPLC purification provided the final construct 5 in >90% purity and ~50% yield over two steps, and its identity was confirmed via MALDI-TOF MS. Among all phalloidin side chains, the position-7 Leu-(OH)₂ side chain is least important for binding to F actin (31). Therefore, the short linker attaching aph to pHLIP-Cys in construct 5 is expected to have only a minimal effect on F-actin binding after release into the cytoplasm.

However, to our surprise, we could not find conditions under which the pHLIP-C(aph) construct stopped or suppressed growth in several cancer cell lines, including HeLa, JC, PC-3, and MCF-7 (see Fig. 2E for data with JC). Furthermore, pHLIP-C(aph) did not induce the expected cytotoxic effects, such as multinucleation or cytoskeleton rigidification, which were observed with the previous construct pHLIP-S-S-(phalloidin-TRITC) (20). Why does pHLIP translocate phalloidin-TRITC into cells more effectively than phalloidin alone? One possible explanation is that the hydrophobic rhodamine dye (i.e., TRITC) renders phalloidin-TRITC less polar than phalloidin, thus reducing the energetic barrier for translocation. Indeed, *n*-octanol/water partition experiments indicate that phalloidin-TRITC is extracted into the *n*-octanol phase ~40× more readily than phalloidin, with a LogP value of -0.05 compared to -1.5 for phalloidin (Fig. 1). If we consider the contribution of linker structures to cargo polarity, the LogP difference between the two cargos could be even more pronounced, because the aryl azide photo-cross-linker used in pHLIP-S-S-(phalloidin-TRITC) is more hydrophobic than the SPDP-derived linker in pHLIP-C(aph). In short, we hypothesized that the hydrophobicity of the cargo correlates with the efficiency of pHLIP-mediated translocation and, in turn, the ability to induce biological effects in cells. To test this idea, we synthesized the pHLIP-K(rho)C(aph) construct 6, in which a rhodamine (rho) moiety [i.e., tetramethylrhodamine (TAMRA)] is placed on a Lys residue inserted immediately preceding the Cys residue carrying phalloidin (Fig. 1). We designed this construct so that the combined hydrophobicity of phalloidin and TAMRA should

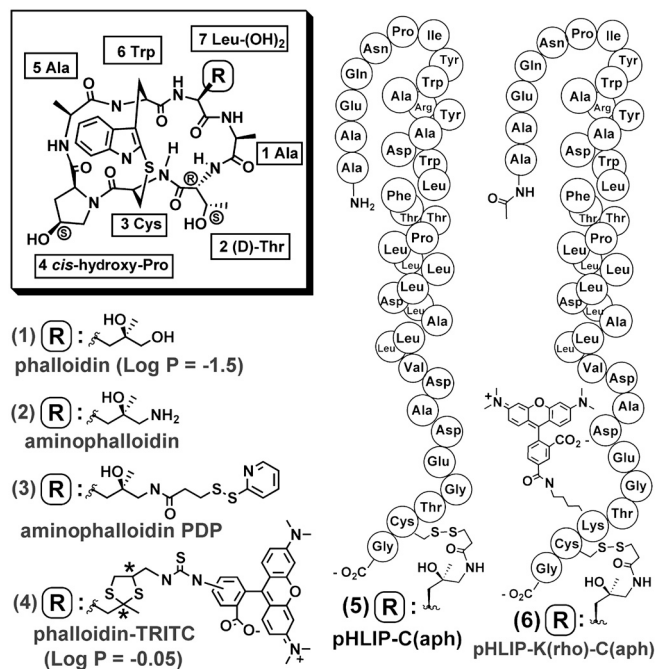


Fig. 1. Phalloidin and pHLIP constructs. Structures of phalloidin and its derivatives are shown as 1–4. For phalloidin-TRITC 4, a star (*) denotes a carbon center of mixed or unspecific stereochemistry. Structures of pHLIP delivery constructs tested in this study are shown as 5 and 6.

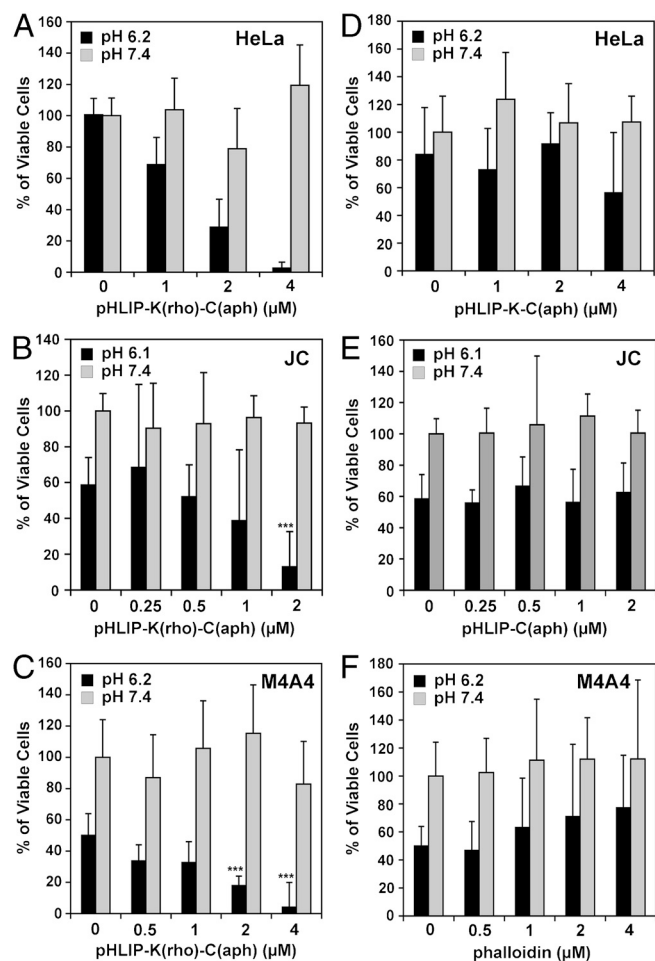


Fig. 2. Studies of growth inhibition by different phalloidin delivery constructs. (A) Phalloidin delivery construct pHLIP-K(rho)C(aph) inhibits the proliferation of HeLa cells in a pH-dependent fashion. HeLa cells in 96-well plates (~4,000 cells per well) were incubated with 1, 2, or 4 μM of pHLIP-K(rho)C(aph) for 3 h at pH 6.2 (black bars) or 7.4 (gray). After 4 d of growth, the number of cells was estimated using the 3-(4,5-dimethylthiazol-2-yl)-5-(3-carboxymethoxyphenyl)-2-(4-sulfophenyl)-2H-tetrazolium inner salt reagent (with OD at 490 nm as readout). All OD at 490 nm readings are normalized to the DMSO control (0 μM , pH 7.4) as 100%, which is ~60,000 to 70,000 cells per well. Errors of the mean were estimated at the 95% confidence level using the two-tailed Student *t* distribution coefficient ($n = 12$ except $n = 4$ for 4 μM at pH 7.4; see *S1 Text* for more details). (B) Inhibition of proliferation of JC cells by pHLIP-K(rho)-C(aph) at pH 6.1 ($n = 4$ except $n = 8$ for 0 μM data). A two-tailed Student *t* test with unequal variance (heteroscedastic) was carried out for the comparison of 0 and 2 μM pH 6.1 datasets (** p value = 0.00071). (C) Inhibition of proliferation of M4A4 cells by pHLIP-K(rho)-C(aph) at pH 6.2 ($n = 4$ except $n = 8$ for 0 μM data). Two pairs of pH 6.2 datasets were compared: 0 vs. 2 μM (** p value = 0.00063) and 0 vs. 4 μM (** p value = 0.00015). (D) HeLa cells were treated with pHLIP-K-C(aph) ($n = 4$), and antiproliferative effect was not observed. (E) pHLIP-C(aph) does not inhibit the proliferation of JC cells ($n = 4$ except $n = 8$ for 0 μM). (F) Phalloidin alone does not inhibit the proliferation of M4A4 cells ($n = 4$ except $n = 8$ for 0 μM).

be similar to that of phalloidin-TRITC. The pHLIP-K-C(aph) intermediate (without the rho moiety) is synthesized and purified in the same fashion as described above for pHLIP-C(aph) **5**. By capping the amino terminus with an acetyl group (during the solid-phase synthesis of the pHLIP-KC peptide), the rho moiety is then selectively conjugated to the Lys side chain using the succinidyl ester of 5-TAMRA. This sequence provides the final construct pHLIP-K(rho)C(aph) **6** in ~27% overall yield in three steps.

Antiproliferative Effects of pHLIP-K(rhodamine)C(aminophalloidin). When HeLa cells were treated with pHLIP-K(rho)C(aph) for 3 h at pH 6.2 (37 °C), cell proliferation was severely disrupted (Fig. 2A). Treatments were carried out at delivery construct concentrations ranging from 1 to 4 μM , in 96-well plates with ~4,000 cells per well. After 4 d of subsequent growth at normal pH, wells treated with 4 μM of pHLIP-K(rho)C(aph) contained almost no viable cells. Up to 97% inhibition of cell growth was achieved. Meanwhile, cells treated with only DMSO (0 μM column in Fig. 2A) had proliferated to ~60,000 cells per well. The antiproliferative effect is concentration dependent: When HeLa cells were treated at 1 and 2 μM concentrations, 31% and 71% inhibitions were observed, respectively. As expected, inhibition of cell growth is pH dependent: Treatment with pHLIP-K(rho)C(aph) at pH 7.4 under the same conditions had no effect on cell proliferation (Fig. 2A). This lack of antiproliferative effects at pH 7.4 is consistent with the notion that delivery of phalloidin is mediated by pH-dependent pHLIP insertion across the plasma membrane, and does not involve endocytosis, which is expected to occur readily at pH 7.4. The low pH treatment in itself did not have any deleterious effect on the proliferation of HeLa cells, as shown by control experiments without pHLIP-K(rho)C(aph) [(Fig. 2A) compare the 0 μM , pH 6.2, black bar with the 0 μM , pH 7.4, gray bar, there is no significant difference].

To check for cell-specific effects, we tested pHLIP-K(rho)C(aph) using JC (mouse mammary gland adenocarcinoma) and M4A4 (human breast ductal carcinoma) cells (Fig. 2B and C). In order to inhibit JC cell growth, the pH of the incubation media had to be further lowered to pH 6.1. The JC and M4A4 cells were more sensitive to low pH than HeLa cells, evidenced by nonspecific cell death at pH 6.1–6.2 that reduced the number of viable cells by ~40–50% (Fig. 2B and C; 0 μM , black bar vs. gray bar). Nonetheless, growth inhibition specific to the presence of pHLIP-K(rho)C(aph) is evident: Treatment with 2 μM of pHLIP-K(rho)C(aph) inhibited 78% of JC proliferation (Fig. 2B, pH 6.1 black bars; 2 vs. 0 μM), whereas 92% inhibition of M4A4 proliferation was observed at 4 μM (Fig. 2C, pH 6.2 black bars; 4 vs. 0 μM). Compared to the 0 μM controls at pH 6.2, reductions in the growth of JC and M4A4 cells are statistically highly significant (p value < 0.001) even at 2 μM of delivery construct. Because some of these cells are already compromised by acidity at pH 6.1–6.2, pHLIP-delivered phalloidin molecules may further tip the balance toward cell death. In short, the antiproliferation effects observed with HeLa cells are reproducible with JC and M4A4 cells.

As expected, under equivalent conditions phalloidin (or aminophalloidin) showed no inhibitory effect on M4A4/HeLa proliferation (Fig. 2F, data for phalloidin with M4A4 cells shown), consistent with the knowledge that phalloidin is a cell-impermeable toxin (30, 31). The rhodamine moiety on pHLIP-K(rho)C(aph) is necessary for inhibition, because (i) under the same conditions pHLIP-C(aph) **5** does not stop the growth of JC or HeLa cells (Fig. 2E, data with JC cells shown); and (ii) no inhibitory effect was observed when HeLa cells were treated with pHLIP-K-C(aph)—a construct missing the rhodamine moiety but otherwise identical to pHLIP-K(rho)C(aph) (Fig. 2D). However, in the case of pHLIP-K-C(aph), we cannot rule out the possibility that the positively charged free Lys side chain in the C terminus further burdens pHLIP insertion, blocking cargo entry. Furthermore, when HeLa cells were treated with an unmodified, “native” pHLIP peptide that does not contain Lys or Cys in its C terminus (thus with no rhodamine or phalloidin cargo attached), no inhibition of proliferation was observed (Fig. S1). Hence, pHLIP insertion in itself does not hinder cell growth, consistent with our previous observations that pHLIP is minimally toxic (20, 21). In summary, these data support our hypothesis that the combined hydrophobicity of the cargos, manifested as an

overall property of the inserting C terminus of pHLIP with its cargo, determines the efficiency of delivery into cells.

Morphological Changes of Cells Treated with pHLIP-K(rhodamine)C (aminophalloidin). As observed previously [in cells incubated with the heterogeneous pHLIP-S-S-(phalloidin-TRITC) construct], HeLa cells treated with pHLIP-K(rho)C(aph) showed signs of cytoskeletal immobilization. After incubation with 4 μ M of pHLIP-K(rho)C(aph) HeLa pH 6.1 for 3 h, HeLa (Fig. 3) or M4A4 (Fig. S2) cells exhibited a reduced ability to contract and “round up” when trypsinized, whereas cells treated at pH 7 detached and rounded as expected (Fig. 3). A subpopulation of the cells treated at low pH also became multinucleated (Fig. 4). Both observations are consistent with a view that pHLIP-K(rho)C(aph) delivers the toxic cargo across the plasma membrane, and that the released phalloidin binds to actin filaments to stabilize them, interfering with the F-actin turnover required both for cytokinesis and for cell contraction.

Discussion

We have studied the use of pHLIP to deliver otherwise cell-impermeable agents across membranes, anticipating that success might expand opportunities for the delivery of therapeutic molecules to treat cancer. We find that pHLIP-mediated translocation of phalloidin can inhibit the proliferation of cancer cells in a pH-dependent fashion. A single 3 h treatment with 4 μ M of delivery construct pHLIP-K(rho)C(aph) at pH 6.1–6.2 led to more than 90% inhibition of HeLa and M4A4 cell growth, and the antiproliferative effect is absent at pH 7.4. Treated cells also showed signs of cytoskeletal immobilization and multinucleation, consistent with the expected binding of phalloidin to F actin, stabilizing the filaments against depolymerization.

The level of inhibition of cell proliferation should be directly correlated with the amount of phalloidin translocated by pHLIP into cells. Actin is one of the most abundant proteins in eukaryotic cells, with a cytoplasmic concentration reaching 63 μ M in fission yeast (or \sim 1.4 million monomers for a 92 μ m³ cell, counting both F and G actin) (33), and the local actin concentration can be as high as 460 μ M in the division site (i.e., the mature contractile ring of fission yeast undergoing cytokinesis) (33) and 650 μ M in lamellipodia of mouse melanoma cells (34). In this respect,

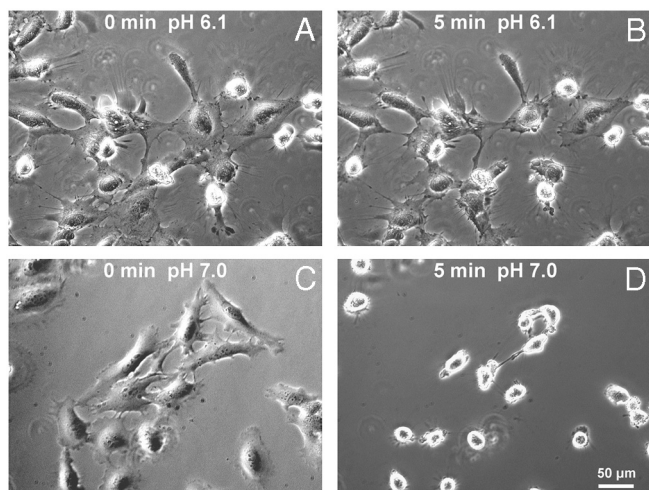


Fig. 3. Trypsinization experiments. Following incubation with pHLIP-K(rho)C(aph) (4 μ M, 3 h) at pH 7, HeLa cells rounded and dissociated quickly after trypsinization: Compare phase contrast image C taken before trypsinization with image D of the same view taken 5 min after addition of trypsin/EDTA. In contrast, HeLa cells treated with pHLIP-K(rho)C(aph) at pH 6.1 (also 4 μ M, 3 h) could not easily contract—a sign of cytoskeleton rigidification, evident from images taken before (A) and 5 min after (B) the addition of trypsin/EDTA solution.

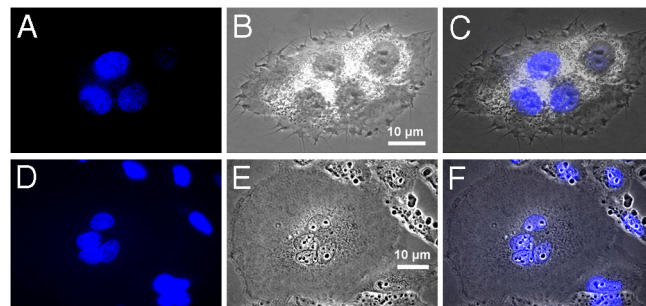


Fig. 4. Multinucleation in treated cells. HeLa and M4A4 cells were treated with pHLIP-K(rho)C(aph) at 4 μ M, pH 6.2 for 3 h. After 2–3 d of growth, a subpopulation of the treated cells became multinucleated. (A) DAPI (4',6-diamidino-2-phenylindole) fluorescence image (artificial blue color) of a M4A4 cell with four nuclei (DAPI binds strongly to dsDNA and selectively stains the nucleus). (B) Phase contrast image of the same multinucleated M4A4 cell. (C) Overlay of images A and B. (D) DAPI fluorescence image of a HeLa cell with four nuclei. (E) Phase contrast image of the same HeLa cell, showing an unusually large volume of cytoplasm. (F) Overlay of D and E. These images were taken using an epifluorescence inverted microscope (Olympus IX71) with a 100 \times objective lens.

targeting actin sets a stringent test for the delivery potential of pHLIP in general. How many copies of toxin can pHLIP deliver per cell? What maximum intracellular toxin concentration can pHLIP build up? And, more specifically, what critical intracellular concentration of phalloidin must have been delivered by pHLIP-K(rho)C(aph) in order to disrupt cell proliferation?

Although we do not know the exact amount of phalloidin delivered by our construct, it is possible to calibrate the levels of cell growth inhibition obtained with pHLIP-K(rho)C(aph) using the known antiproliferative effects of phalloidin. Weber and coworkers showed that in order to delay or stop the proliferation of PtK2 cells (rat kangaroo kidney epithelium), a microinjection of a phalloidin stock solution of 0.2 or 1 mM is required, respectively, probably leading to 20–100 μ M intracellular phalloidin concentration (approximately 1:1 ratio to cytoplasmic actin) (30). Thus, by analogy, treatments with pHLIP-K(rho)C(aph) at 2–4 μ M also seem able to build up cytoplasmic phalloidin concentration in the 20–100 μ M range. We estimate that this level of toxin buildup requires pHLIP to deliver 21–106 million phalloidin molecules per cell, calculated for HeLa cells in suspension with a 15- μ m average diameter (1,767 μ m³ volume) (Fig. 3), which in turn, implies that pHLIP-K(rho)C(aph) occupies roughly 1–7% of the plasma membrane area available for insertion in the attached cell (taking a pHLIP cross-section area of \sim 113 Å^2 in the inserted state, and an available cell surface area of 1,800 μ m², estimated from Fig. 3). Thus, perhaps a near-saturating level of inserted pHLIP-K(rho)C(aph) is needed to build up a 100 μ M intracellular concentration of cargo, which likely represents an upper limit of what is possible with pHLIP-mediated delivery.

In addition, we studied the insertion behavior of pHLIP-K(rho)C(aph) into liposomes (see *SI Text* for details). By following changes in Trp fluorescence, we deduced that pHLIP-K(rho)C(aph) inserts into 1-palmitoyl-2-oleoyl-sn-glycero-3-phosphocholine (POPC) lipid bilayers with an apparent pK_a of \sim 6.16 (Fig. S3). This value is similar to that of the parent pHLIP peptide (without any cargo) (16) and consistent with the level of acidity required for antiproliferative effects in cell experiments (i.e., pH 6.1–6.2). Further, sedimentation velocity experiments showed that pHLIP-K(rho)C(aph) is predominantly monomeric (>90%) in solution under conditions employed to treat cells (i.e., pH 6.2, 4 μ M, physiological ionic strength) (Fig. S4).

To facilitate phalloidin delivery, a lipophilic rhodamine moiety is also attached to the inserting end of pHLIP-K(rho)C(aph). An antiproliferative effect was not observed without the hydrophobic

facilitator. Liposome studies showed that the failed construct pHLP-C(aph) also seems able to insert into POPC membranes with a pK_a of ~ 6.14 (see *SI text* and *Fig. S3*) and it is also predominantly monomeric ($>80\%$) at $4 \mu\text{M}$ concentration, pH 6.2 (*Fig. S4*). However, we cannot exclude the possibility that during insertion pHLP-C(aph) is trapped in a partially inserted intermediate and no translocation of cargo occurs (see *SI text* for further discussion). It is also possible that there is a property (or a set of properties) that alters delivery efficiency in cells between these two constructs, but not in vesicles, resulting in an insufficient amount of phalloidin delivered by pHLP-C(aph). Possible factors include kinetic differences in the association with and/or insertion into the plasma membrane, influenced by parameters present only in the cells, such as the membrane potential, cholesterol content, membrane protein content, surface glycosylation, and other lipid compositional variables. Further work will be needed to explore such factors.

In summary, we showed that pHLP-K(rho)C(aph) can deliver enough phalloidin molecules to kill cancer cells in vitro at pH 6.2 but has no effect on cells at neutral pH. This work opens unexplored avenues of investigation to evolve antitumor agents that preferentially destroy cancer cells in acidic solid tumors, while minimally affecting cells in normal tissues, and to use therapeutic molecules that do not enter cells on their own.

Materials and Methods

A more detailed description of the antiproliferative assays, as well as experimental procedures of the syntheses of pHLP-C(aph) and pHLP-K(rho)C(aph), cell culture, cell morphology assays and microscopy, liposome preparation,

Trp fluorescence spectroscopy, analytical ultracentrifugation (sedimentation velocity experiments), LogP measurements, and information about data analysis and the stability of delivery constructs are available online in the *SI Text*.

Stock solutions of pHLP-C(aph) 5, pHLP-K(rho)C(aph) 6, phalloidin 1, pHLP-K-C(aph) and pHLP were prepared in DMSO at $200 \mu\text{M}$ concentration. HeLa, JC, or M4A4 cells were seeded in 96-well plates (Costar) at a density of $\sim 1,000$ cells per well, and then grown for 2 d before treatment. DMSO stock of pHLP-K(rho)C(aph) (or a control agent) was diluted with pH-adjusted, sterile Leibovitz's L-15 Phenol Free Medium (L-15) to give treatment solutions in the $0.25\text{--}4 \mu\text{M}$ range. Appropriate amounts of DMSO were added to ensure that all treatment samples contain $\sim 2\%$ by volume. After removal of cell media, the L-15 treatment solution was added to each well (volume for HeLa plate, $80 \mu\text{L}$ per well; JC and M4A4, $160 \mu\text{L}$), and then the plate was incubated at 37°C for 3 h. To minimize week-to-week cell variability, treatments at pH 6.1–6.2 and 7.4 were carried out on the same 96-well plate and all negative control data shown (in *Fig. 2 D–F* and *Fig. S1*) are from plates in which positive results were also obtained. After treatment, $200 \mu\text{L}$ of normal media was added to each well before returning the plate to the incubator. Cell density of the "0 μM , pH 7.4" controls usually reached 40,000–80,000 cells per well after 3–6 d of growth. The viable cell number was quantified using the 3-(4,5-dimethylthiazol-2-yl)-5-(3-carboxymethoxyphenyl)-2-(4-sulfophenyl)-2H-tetrazolium inner salt reagent (Promega CellTiter 96 Aqueous One Solution Cell Proliferation Assay). OD at 490 nm values were obtained using a plate reader (Spectramax M2 from Molecular Devices).

ACKNOWLEDGMENTS. The authors thank Dr. Lan Yao (Department of Physics, University of Rhode Island) and Dr. William H. Brissette for their important experimental advice. We also thank Dr. Damien Thevenin and Dr. Francisco Barrera Olivares for discussions and comments on the manuscript. This work was supported by National Institutes of Health Grants GM073857 (to D.M.E.) and CA133890 (to O.A.A., D.M.E., and Y.K.R.), and by an Anna Fuller Fund Postdoctoral Fellowship in Molecular Oncology (M.A.).

- Matsumura Y, Maeda H (1986) A new concept for macromolecular therapeutics in cancer chemotherapy: Mechanism of tumortropic accumulation of proteins and the antitumor agent SMANCS. *Cancer Res* 46:6387–6392.
- Maeda H, Bharate GY, Daruwalla J (2009) Polymeric drugs for efficient tumor-targeted drug delivery based on EPR-effect. *Eur J Pharm Biopharm* 71:409–419.
- Jain RK (1987) Transport of molecules in the tumor interstitium: A review. *Cancer Res* 47:3039–3051.
- Sarapa N, et al. (2003) Assessment of normal and tumor tissue uptake of MAG-CPT, a polymer-bound prodrug of camptothecin, in patients undergoing elective surgery for colorectal carcinoma. *Cancer Chemother Pharmacol* 52:424–430.
- Yuan F, et al. (1994) Vascular permeability and microcirculation of gliomas and mammary carcinomas transplanted in rat and mouse cranial windows. *Cancer Res* 54:4564–4568.
- Allen TM, Cullis PR (2004) Drug delivery systems: Entering the mainstream. *Science* 303:1818–1822.
- Allen TM (2002) Ligand-targeted therapeutics in anticancer therapy. *Nat Rev Cancer* 2:750–763.
- Low PS, Kularatne SA (2009) Folate-targeted therapeutic and imaging agents for cancer. *Curr Opin Chem Biol* 13:256–262.
- Hynes NE, Lane HA (2005) ERBB receptors and cancer: The complexity of targeted inhibitors. *Nat Rev Cancer* 5:341–354.
- Fox EJ, Salk JJ, Loeb LA (2009) Cancer genome sequencing—an interim analysis. *Cancer Res* 69:4948–4950.
- Li C, et al. (2007) Identification of pancreatic cancer stem cells. *Cancer Res* 67:1030–1037.
- Hambley TW, Hait WN (2009) Is anticancer drug development heading in the right direction? *Cancer Res* 69:1259–1262.
- Gerweck LE, Seetharaman K (1996) Cellular pH gradient in tumor versus normal tissue: Potential exploitation for the treatment of cancer. *Cancer Res* 56:1194–1198.
- Makovitzki A, Fink A, Shai Y (2009) Suppression of human solid tumor growth in mice by intratumor and systemic inoculation of histidine-rich and pH-dependent host defense-like lytic peptides. *Cancer Res* 69:3458–3463.
- Zhang X, Lin Y, Gillies RJ (2010) Tumor pH and its measurement. *J Nucl Med* 51:1167–1170.
- Hunt JF, Rath P, Rothschild KJ, Engelman DM (1997) Spontaneous, pH-dependent membrane insertion of a transbilayer alpha-helix. *Biochemistry* 36:15177–15192.
- Reshetnyak YK, Segala M, Andreev OA, Engelman DM (2007) A monomeric membrane peptide that lives in three worlds: In solution, attached to, and inserted across lipid bilayers. *Biophys J* 93:2363–2372.
- Reshetnyak YK, Andreev OA, Segala M, Markin VS, Engelman DM (2008) Energetics of peptide (pHLIP) binding to and folding across a lipid bilayer membrane. *Proc Natl Acad Sci USA* 105:15340–15345.
- Zoonens M, Reshetnyak YK, Engelman DM (2008) Bilayer interactions of pHLIP, a peptide that can deliver drugs and target tumors. *Biophys J* 95:225–235.
- Reshetnyak YK, Andreev OA, Lehnert U, Engelman DM (2006) Translocation of molecules into cells by pH-dependent insertion of a transmembrane helix. *Proc Natl Acad Sci USA* 103:6460–6465.
- Andreev OA, et al. (2007) Mechanism and uses of a membrane peptide that targets tumors and other acidic tissues in vivo. *Proc Natl Acad Sci USA* 104:7893–7898.
- Andreev OA, et al. (2010) pH (low) insertion peptide (pHLIP) inserts across a lipid bilayer as a helix and exits by a different path. *Proc Natl Acad Sci USA* 107:4081–4086.
- Vavere AL, et al. (2009) A novel technology for the imaging of acidic prostate tumors by positron emission tomography. *Cancer Res* 69:4510–4516.
- Segala J, Engelman DM, Reshetnyak YK, Andreev OA (2009) Accurate analysis of tumor margins using a fluorescent ph-(low)-insertion-peptide (pHLIP). *Int J Mol Sci* 10:3478–3487.
- Thevenin D, An M, Engelman DM (2009) pHLIP-mediated translocation of membrane-impermeable molecules into cells. *Chem Biol* 16:754–762.
- Torchilin VP (2006) Recent approaches to intracellular delivery of drugs and DNA and organelle targeting. *Annu Rev Biomed Eng* 8:343–375.
- Wieland T (1977) Modification of actins by phallotoxins. *Naturwissenschaften* 64:303–309.
- Faulstich H, Schafer AJ, Weckauf M (1977) The dissociation of the phalloidin-actin complex. *h-s Z Physiol Chem* 358:181–184.
- De La Cruz EM, Pollard TD (1994) Transient kinetic analysis of rhodamine phalloidin binding to actin filaments. *Biochemistry* 33:14387–14392.
- Wehland J, Osborn M, Weber K (1977) Phalloidin-induced actin polymerization in the cytoplasm of cultured cells interferes with cell locomotion and growth. *Proc Natl Acad Sci USA* 74:5613–5617.
- Wulf E, Deboben A, Bautz FA, Faulstich H, Wieland T (1979) Fluorescent phalloidin, a tool for the visualization of cellular actin. *Proc Natl Acad Sci USA* 76:4498–4502.
- Wieland T, Hollosi M, Nassal M (1983) Components of the green deathcap mushroom (*Amanita phalloides*), LXI: delta-Aminophalloin, a 7-analogue of phalloidin, and some biochemically useful, including fluorescent derivatives. *Liebigs Ann Chem* 1983:1533–1540.
- Wu JQ, Pollard TD (2005) Counting cytokinesis proteins globally and locally in fission yeast. *Science* 310:310–314.
- Koestler SA, et al. (2009) F- and G-actin concentrations in lamellipodia of moving cells. *PLoS One* 4:e4810.